Archive of bacterial community in anhydrite crystals from a deep-sea basin provides evidence of past oil-spilling in a benthic environment in the Red Sea

Yong Wang[1,2], Tie Gang Li[3,4], Meng Ying Wang[1], Qi Liang Lai[5], Jiang Tao Li[6], Zhao Ming Gao[1], Zong Ze Shao[5], Pei-Yuan Qian[2,*]

[1]Institute of Deep-Sea Science and Engineering, Chinese Academy of Sciences, San Ya, China

[2] Division of Life Science, Hong Kong University of Science and Technology, Clear Water Bay, Hong Kong, China

[3] Key Laboratory of Marine Sedimentology and Environmental Geology, First Institute of Oceanography, State of Oceanic Administration (SOA), Qingdao, China

[4]Laboratory for Marine Geology, Qingdao National Laboratory for Marine Science and Technology, Qingdao, China

[5] Key Laboratory of Marine Biogenetic Resources, The Third Institute of Oceanography, SOA, Xiamen, China

[6] State Key Laboratory of Marine Geology, Tongji University, Shanghai, China

Corresponding author: boqianpy@ust.hk, Tel: 852-2358-7331

Keywords: *Alcanivorax*; metagenome; anhydrite; Atlantis II brine pool; hydrothermal sediment

Running title: Archive of microbial inhabitants in anhydrites

25 **Abstract**

26 In deep-sea sediment, the microbes present in anhydrite crystals are potential markers of

27 the past environment. In the Atlantis II Deep, anhydrite veins were produced by mild

28 mixture of calcium-rich hydrothermal solutions and sulfate in the bottom water, which

29 had probably preserved microbial inhabitants in the past seafloor of the Red Sea. In this

30 study, this hypothesis was tested by analyzing the metagenome of an anhydrite crystal

31 sample from the Atlantis II Deep. The estimated age of the anhydrite layer was between

32 750-770 years, which might span the event of hydrothermal eruption into the benthic

33 floor. The 16S/18S rRNA genes in the metagenome were assigned to Bacteria, Archaea,

34 Fungi and even invertebrate species. The dominant species in the crystals was an

35 oil-degrading *Alcanivorax borkumensis* bacterium, which was not detected in the adjacent

36 sediment layer. Fluorescence microscopy using 16S rRNA and marker gene probes

37 revealed intact cells of the *Alcanivorax* bacterium in the crystals. A draft genome of *A.*

38 *borkumensis* was binned from the metagenome. It contained all functional genes for

39 alkane utilization and the reduction of nitrogen oxides. Moreover, the metagenomes of

40 the anhydrites and control sediment contained aromatic degradation pathways, which

41 were mostly derived from *Ochrobactrum* sp. Altogether, these results indicate an oxic,

42 oil-spilling benthic environment in the Atlantis II basin of the Red Sea in approximately

43 the 14th century. The original microbial inhabitants probably underwent a dramatic

44 selection process via drastic environmental changes following the formation of an

45 overlying anoxic brine pool in the basin due to hydrothermal activities.

46

47

48

1. Introduction

Deep-sea sediment is among the least explored biospheres on Earth. Indigenous microbes differ vastly in community composition and metabolic spectra at different depths and sites (Orcutt et al., 2011;Teske and Sorensen, 2007). The distribution of microbes in subsuperficial sediments is determined by the porosity, nutrient availability and geochemical conditions of the sediment (Parkes et al., 2000;Webster et al., 2006). In return, genomic features and the community composition of the indigenous microbial inhabitants may reflect the *in situ* conditions and serve as biomarkers containing the geochemical indicators. However, most of the biomarkers cannot be well preserved and will be degraded by biological and abiological activities. Although lipids and other organic carbons present in some minerals allow the interpretation of microbial activities to some extent (Brocks et al., 2005), the original metabolic activities are difficult to retrieve in a comprehensive and precise manner.

Most of the dead microbes are damaged during the sedimentation process, but some can be maintained in almost their original shape (Taher, 2014;Benison et al., 2008). Evaporites, which mostly consist of halite and anhydrite ($CaSO_4$) or gypsum ($CaSO_4 \cdot 2H_2O$, temperature <38℃ (Hill, 1937)), are common microbialites with accretionary organosedimentary structures (Dupraz et al., 2011). Numerous dead bacteria, algae and metazoans have been detected in gypsum granules (Petrash et al., 2012;Trichet et al., 2001); bacterial mats growing on evaporites may become trapped and constitute much larger microbialites (Babel, 2004). Consequently, microbial inhabitants on the benthic surface may get trapped in the evaporites (Benison et al., 2008). Anhydrite facies are not found throughout deep-sea sediments. They usually form around hydrothermal vents in deep-sea environments (Jannasch and Mottl, 1985). A strong deep-sea volcanic eruption may break the crustal basalts, resulting in a drastic emission of hydrothermal gases followed by the crystallization of anhydrites and the deposition of metal sulfides (Kristall et al., 2006). An alternative model is that mild hydrothermal activities lead to a slow influx of solutions into the overlying sediment at temperatures in the sub-seafloor ranging from 20-100℃. This process also results in the formation of crystalline anhydrites in veins and around warm vents (Jannasch and Mottl, 1985). The latter process

80   may trap microbial inhabitants on the seafloor and within surface layers in anhydrites.

81   Due to the mild temperature, the trapped bodies are better preserved as excellent

82   biological evidence for past geochemical conditions.

83

84   A similar mild hydrothermal field is present in the Red Sea. Initially found in a deep-sea

85   rift in the 1960s (Swallow and Crease, 1965;Girdler, 1970), the temperature of the

86   Atlantis II brine pool has recently increased to 68°C (Anschutz and Blanc, 1996). In 1972,

87   several sediment cores were obtained from the southwest region of the pool (DSDP

88   Site226), and metal sulfides and evaporites were recognized as major mineral facies in

89   this brine-filled basin (Party, 1974). In particular, thick and well-crystalized anhydrite

90   layers were found within the hematite and at the bottom of the cores. Two major

91   anhydrite units were later defined by analysis of the adjacent core samples. The lower

92   unit comprised anhydrite ranging from 12 to 70 wt% (Anschutz et al., 2000). The

93   anhydrite in the sediments likely resulted from a geyser-type eruption of hydrothermal

94   solutions into the Atlantis II brine pool followed by the mixing of calcium-rich solutions

95   with dissolved sulfate-bearing brine and the precipitation of anhydrites during the cooling

96   process (Ramboz et al., 1988). The discovery of veins containing sulfides and anhydrite

97   in the sediment suggests that a mild hydrothermal eruption created the anhydrite facies in

98   the Atlantis II sediment (Zierenberg and Shanks, 1983;Oudin et al., 1984;Missack et al.,

99   1989). The formation of anhydrite facies in this manner would trap microbial cells and

100   organic debris in the bottom water and surface sediment. These anhydrite layers probably

101   contained important indigenous microbial inhabitants during the occurrence of the

102   hydrothermal events at the deep-sea benthic floor of the Red Sea. Coupled with [14]C

103   markers to estimate age, the anhydrite facies contained a large quantity of information

104   regarding the past geochemical changes. The formation process of the Atlantis II brine

105   pool is still controversial, largely because the source of the brine is uncertain (Schardt,

106   2016). The brine water had converted the bottom of the deep into anoxic, hypersaline and

107   hot environment. The microbes in the anhydrite facies may provide hints for the original

108   benthic conditions and age of the pool. It is also an interesting question whether oil was

109   generated in the sediments under the mild hydrothermal activities in the past deep. If yes,

110 seeping hydrothermal solutions may bring oil into the seafloor of the deep, which might

111 be documented by the microbes in the anhydrites.

112

113 In the present study, we sampled a sediment core near Site226 and detected an anhydrite

114 layer. The dominant species were alkane- and oil-degrading bacteria indicating an oxic,

115 oil-spilling benthic condition when the layer was formed. The present study sheds light

116 on the importance of anhydrites in deep-sea sediment as an archive of microbial

117 inhabitants that can serve as biomarkers of past geochemical events.

118

2   Materials and methods

119

2.1 Physicochemical measurements of sediment layers

120

121 In 2008, a 2.25-meter gravity sediment core was obtained from the southwest basin

122 (approximately 2180 meters below sea level) of the Atlantis II Deep (21°20.76' N,

123 38°04.68' E) in the Red Sea (Fig. S1) (Bower, 2009). The core was frozen at -80°C and

124 then sliced aseptically into seventy-five 3-cm sections. Microbes from sediment slices of

125 12-15 cm, 63-66 cm, 105-108 cm, 183-186 cm, and 222-225 cm were first suspended in

126 phosphate-buffered saline and shaken on a vortexer for 30 s. After 30 minutes, the

127 supernatant was filtered through a 0.22-μm black polycarbonate filter. After

128 6-diamidino-2-phenyloindole (DAPI) staining, the microbes from each layer were

129 counted under an epifluorescence microscope (n = 3) (Gough and Stahl, 2003). The pore

130 water from the above 5 layers was collected by centrifugation. The concentration of

131 dissolved organic carbon (DOC) in the pore water was determined using the combustion

132 method (Trichet et al., 2001). The concentrations of ammonium, nitrite and nitrate were

133 measured using a TNM-I analyzer (Simadzu, Kyoto, Japan). To separate large particles

134 (>63 μm) from small particles (<63 μm), the sediment samples were passed through a

135 63-μm stainless steel sieve. The percentage of small particles (dry weight) was calculated

136 for all slices.

137

138 The age of the sections was estimated with a radiometric dating method that utilizes the

139 naturally occurring radioisotope [14]C. The monospecific *Globigerinoides sacculifer*

140 specimens ranging in size from 250 to 350 μm were manually selected with caution and

141   then subjected to ^{14}C measurement in the National Ocean Sciences Accelerator Mass

142   Spectrometry (AMS) Facility at the Woods Hole Oceanographic Institute, USA. The raw

143   AMS ^{14}C ages were converted to calendar ages using the CALIB 6.0 program

144   (http://calib.qub.ac.uk/calib/) with the dataset Marine 09 (Reimer et al., 2009). A

145   reservoir correction has been considered for the ^{14}C difference between atmospheric and

146   surface waters (Bard, 1988).

147

148   **2.2 DNA extraction and amplification**

149   The boundary of the anhydrite layer was determined by naked eye observation and

150   particle size measurement. Crystals were manually collected from the layers, followed by

151   ultrasonic cleaning. The homogenized crystals were then analyzed by X-ray

152   diffraction (XRD) (Rigaku, Tokyo, Japan) using Cu K-alpha radiation of 40 kV and 30

153   mA. The following procedure was conducted for DNA extraction from the crystals with

154   caution to avoid contamination. Surface contamination was removed by rinsing with 70%

155   alcohol in autoclaved distilled deionized water, followed by pulsed ultrasonic cleaning

156   for 2 hours. Anhydrite crystals (20 g) (Fig. 1A) of different sizes were treated with 1 µL

157   (2U) Turbo DNase I (Ambion, Austin, Texas, US) for 30 m in a 37℃ incubation before

158   being ground for DNA extraction in a sterile hood. The anhydrite powder was used for

159   DNA extraction with the PowerSoil DNA Isolation kit (MO-BIO, Carlsbad, USA),

160   followed by a purification step according to the manufacturer's instructions. The DNA

161   concentration was quantified with a Quant-iT PicoGreen kit (Invitrogen, USA). Twenty

162   picograms of the raw DNA extract was used for DNA amplification using a MALBAC

163   kit (Yikang, Jiangsu, China) according to the manufacturer's manual (Zong et al., 2012).

164   The MALBAC amplification method has been evaluated recently in metagenomic studies

165   (Wang et al., 2016). Two MALBAC amplification assays were conducted using

166   twenty-one PCR cycles to acquire a sufficient amount of DNA for subsequent sequencing.

167   A negative control was also incorporated in the assay. The DNA concentration of the

168   MALBAC-amplified sample and the negative control was measured with a Bioanalyzer

169   (Agilent, CA, US). The products of the MALBAC amplification and negative control

170   were examined by gel electrophoresis to confirm the size ranges of the amplicons. Three

171   replicates of MALBAC amplifications for each sample were mixed and used for Illumina

172 sequencing on a Hiseq2000 platform (Illumina, San Diego, US). As a control, 10 g of

173 sediment from a position at 168 cm from the top of the core was used for DNA extraction.

174 There were no recognizable anhydrite crystals in this layer. DNA sequencing was

175 conducted as described above.

176

2.2 Binning of metagenomes

178 The initial Illumina 2×110-bp paired-end reads were subjected to quality assessments

179 using the NGS QC Toolkit with default parameters (Patel and Jain, 2012). The Illumina

180 sequencing data were deposited in the NCBI SRA database (accession number

181 SRA356974). The 35-bp MALBAC adapters at the two ends of the sequencing reads

182 were removed. Assembly of the trimmed Illumina 2×75-bp paired-end reads was

183 performed using SPAdes 3.5 (Nurk et al., 2013). The read coverage for the assembled

184 contigs was calculated using SAMtools (Li et al., 2009). The 16S/18S rRNA genes in the

185 contigs were identified using rRNA_HMM (Huang et al., 2009). Using classify.seqs

186 command in mothur package (Schloss et al., 2009), taxonomic sorting of the 16S rRNA

187 genes was conducted against the SILVA database with a confidence threshold of 80%.

188 The relative abundance of the species in the metagenomes was roughly estimated based

189 on the coverage of the 16S/18S rRNA genes. Binning of the draft genomes was

190 performed based on the read coverage and G+C content of the contigs (Fig. 1B), followed

191 by principal component analysis (PCA) of the tetranucleotide frequencies (TNF) of their

192 respective contigs using a previously described pipeline (Fig. 1C) (Albertsen et al., 2013).

193 The R scripts for the binning process were obtained from

194 https://github.com/MadsAlbertsen/multi-metagenome. To evaluate the completeness of

195 the draft genome, conserved single-copy genes (CSCGs) were counted in the genome.

196 The CSCGs were identified by searching the CDSs against a database of essential

197 bacterial genes (107 essential genes) (Albertsen et al., 2013) using hmmsearch (3.0) with

198 default cutoffs for each protein family.

199

2.3 Genomic analyses

201 The coding DNA sequences (CDSs) of the draft genome were predicted using Prodigal

202 (version 2.60)(Hyatt et al., 2010). KEGG annotation of the CDSs was performed using

203   BLASTp against the KEGG database (Kanehisa et al., 2012) with a maximum e-value

204   cutoff of 1e-05. The KEGG pathways were reconstructed using the KEGG website

205   (http://www.kegg.jp). CDSs were also annotated against the NCBI NR database, and

206   MEGAN was used for taxonomic affiliation and SEED/subsystem annotation of the

207   CDSs (Overbeek et al., 2005). The draft genome was submitted to NCBI (accession

208   number LKAP00000000). The average nucleotide identity (ANI) was calculated using

209   the algorithm integrated in the web service of EZGenome (Goris et al., 2007). The

210   DNA-DNA hybridization (DDH) estimate value was calculated using the

211   genome-to-genome distance calculator (GGDC2.0) with the alignment method of

212   BLAST+ (Meier-Kolthoff et al., 2013;Auch et al., 2010a;Auch et al., 2010b).

213

214   **2.4 Detection and phylogeny of 16S ribosomal RNA (rRNA) genes**

215   The 16S rRNA gene sequence was identified from the draft genome sequence. The

216   closest relatives based on 16S sequence similarity were determined using the web service

217   of EzTaxon (Kim et al., 2012). The neighbour-joining phylogenetic tree was constructed

218   using MEGA version 5.0 (Tamura et al., 2011) with the Kimura 2-parameter model. The

219   phylogenetic tree was supported with bootstrap values based on 1000 replications.

220

221   **2.5 Fluorescence *in situ* hybridization (FISH) of *Alcanivorax* bacteria**

222   FISH probes for 16S rRNA gene of *Alcanivorax* bacteria were designed based on the 16S

223   rRNA gene sequence extracted from the *Alcanivorax* draft genome. Two 16S rRNA

224   fragments, 5'- CCTCTAATGGGCAGATTC-3' and 5'-CCCCCTCTAATGGGCAGA-3',

225   were selected as candidate probes with Probe_Design in the ARB package (Ludwig et al.,

226   2004). The coverage efficiency of the probes was then examined in the Silva database

227   (Quast et al., 2013). The 6-FAM-labeled probe used to target the *alkB* gene was

228   5'-ATGGAGCCTAGATAATGAAGT-3' (Wang et al., 2010). A pure culture of

229   *Alcanivorax borkumensis* Sk2 was first used to examine the probes before performing the

230   assay, and a culture of *Escherichia coli* was used as a negative control. Two grams of

231   anhydrite crystals were sonicated for 30 min in 1 U DNase I solution. The crystals were

232   washed with deionized water and then ground into a powder with a beadbeater in a

233   germ-free environment. The supernatant was mixed with 37% formaldehyde (final

234 concentration, 1-4%). To fix the cells in PBS buffer, the sample was maintained at 4°C for

235 3-4 hr. After centrifugation at 13,000 r/min for 3 min, the supernatant was discarded. The

236 remaining microbes were soaked in 200 μL of PBS buffer, followed by addition of 200 μL

237 of ethanol (Pernthaler et al., 2002). The sample was filtered through 3-μm and 0.22-μm

238 membranes sequentially (diameter, 25 mm; Millipore, Eschborn, Germany). After

239 dehydration of the membrane using alcohol, 2 μL of dying solution containing

240 oligonucleotide probes and 20 μL of buffer (360 μL of 5 M NaCl,40 μL of 1 M Tris/HCl,

241 700 μL of 100% formamide,2 μL of 10% SDS,and water to a total volume of 2 mL).

242 The hybridization of the probes to the microbes was performed for 2 h at 46°C. Rinsing

243 buffer (700 μL of 5 M NaCl, 1 mL of 1 M Tris/ HCl, 500 μL of 0.5 M EDTA, 50 μL of

244 10% SDS and water to a total volume of 50 mL) was used to remove free probes. For

245 counterstaining, 50 μL of 4', DAPI solution (1 μg/mL) was added to the sample. After

246 incubation for 3 min, the sample was washed in Milli-Q water (MetaPhor Bioproducts,

247 Rockland, Maine) and 96% ethanol for 1 min (Pernthaler et al., 2002). The microscopic

248 observation was conducted using an Olympus BX51 (Olympus, Tokyo, Japan).

249

250 **3 Results**

251 **3.1 Physicochemical profile and cell counts**

252 A thick anhydrite layer was present at the bottom of the sediment core based on

253 naked-eye observation of the color and grain size. The anhydrite layer at depths ranging

254 from 177-198 cm consisted of coarse, agglutinated crystals, which corresponded to the

255 high percentage of large grains (78 wt% larger than 63 μm) (Fig. 2). The XRD analysis

256 further confirmed that the crystals in this layer were anhydrite. In contrast, halite

257 comprised the evaporites at depths of 12 cm, 63 cm, 105 cm and 222 cm. For the samples

258 at different depths, the DOC concentration was measured, and the highest value was

259 recorded at 183 cm (80.9 mg L^{-1}), which was even higher than the surface layer at 12 cm

260 (Fig. 3). In the 12 cm layer, the cell density was 3.2×10^5 cells per cm^3, whereas in the

261 layers at 63 cm, 105 cm and 222 cm, it was reduced by 88%, 92% and 96%, respectively

262 (Fig. 3). The cell density was also calculated as the number of cells per gram of sediment.

263 The results revealed a value of 7.1×10^5 cells per gram at a depth of 12 cm, which declined

264 more than 70% in the deeper layers. Although the cell density in the 183 cm layer

265 (6.7×10^4 cells/cm^3) was markedly lower than that in the 12 cm layer, it was higher than

266 those in the 105 cm and 222 cm layers.

267

268 The sediment as a whole is a highly reductive environment, as indicated by the low

269 nitrate, low nitrite and extremely high ammonium concentrations (Fig. 3). To determine

270 the time of the anhydrite layers at 177-198 cm, an age estimate was performed for several

271 layers. The sediment ages were estimated based on the radioisotope ^{14}C of *G. sacculifer*

272 assuming a linear increment from the top (Fig. 2). The results obtained for the layers

273 above and below the anhydrite layer indicated a narrow range of 750-770 years between

274 153 cm and 198 cm (Table 1).

275

276 **3.2 Draft genome of the dominant bacterial species in anhydrites**

277 About 1.8 Gbp Illumina raw sequencing data were obtained for the anhydrite sample and

278 3.1 Gbp data were obtained for the adjacent control layer. The size of the anhydrite and

279 control metagenomes was 59 and 84 Mbp, respectively, after assembly (Table S1). The

280 microbial communities differed remarkably according to the taxonomic assignment of the

281 16S/18S rRNA gene fragments in the two metagenomes (Fig. 4). At the genus level, only

282 *Ochrobactrum* and *Alkanindiges* were common inhabitants in both samples. *Alcanivorax*

283 and *Bacillus* were also dominant genera in the anhydrite and the control, respectively. At

284 the phylum level, excluding the Proteobacteria, the two metagenomes had distinctive

285 phyla. The anhydrite contained archaea that were represented by the methanogenic

286 *Methanoculleus* (Barret et al., 2012); and fungi that consisted of the Ascomycota. In

287 contrast, the control sediment contained mainly Firmicutes, Bacteroides, Actinobacteria,

288 and Deinococcus-Thermus. At last, an invertebrate species, *Prototritia* sp. belonging to

289 Arthropoda, was identified in the anhydrite.

290

291 **3.3 Genome binning of an *Alcanivorax borkumensis* genome**

292 The binned draft genome from the anhydrite metagenome was 3,069,971 bp and

293 comprised 77 contigs. A partial 16S rRNA gene sequence (805 bp) was extracted from

294 the draft genome. Because the sequence was almost identical to that of *A. borkumensis*

295 Sk2 (99.9%) (see also genomic alignment in Fig. S2), we considered the binned draft

296   genome to be from a strain of *A. borkumensis*. As shown in Figure 5, a phylogenetic tree

297   based on the 16S rRNA gene sequences of the genus *Alcanivorax* indicated that the strain

298   clustered with *A. borkumensis* Sk2, an exclusive and ubiquitous hydrocarbon-degrading

299   bacterium (Schneiker et al., 2006;Sabirova et al., 2011). The strain name of the *A.*

300   *borkumensis* in the sediment core was ABS183. It was the only microbial species that

301   could be reliably separated from the metagenome.

302

303   The genome of *A. borkumensis* ABS183, despite containing gaps, was slightly smaller

304   than that of *A. borkumensis* Sk2 (accession number NC_008260; 3,120,143 bp),

305   suggesting that the draft genome of *A. borkumensis* ABS183 was nearly complete. Also,

306   there were not detectable alignment gaps between the two genomes (Fig. S2). The

307   identification of a complete list of single-copy genes also supported the completeness of

308   the genome. The DDH estimation between *A. borkumensis* ABS183 and Sk2 was

309   97.1%±1.3%, which was higher than the standard cut-off value of 70% for genome

310   relatedness between pairs of species (Wayne et al., 1987). The ANI value between

311   ABS183 and Sk2 was 99.9%, which was also higher than the standard ANI criterion for

312   species identity (95%–96%) (Richter and Rossello-Mora, 2009). These results further

313   confirmed that ABS183 was a strain of *A. borkumensis*.

314

315   The genome of *A. borkumensis* ABS183 contains two copies of the alkane-1

316   monooxygenase gene (*alkA*; 10502_28 and 2890_35), which is an essential functional

317   gene for alkane utilization by *Alcanivorax* bacteria (Fig. 6) (Schneiker et al., 2006).

318   Neighboring the *alkA* genes, *alkBGHJ* genes, a GntR family transcriptional regulator

319   gene, and a rubredoxin gene were identified. The gene order of the related genes was

320   consistent with that of the homologs in the genome of strain Sk2 (Schneiker et al., 2006).

321   The *alk* genes were completely absent from the control metagenome. Moreover, the

322   genome of *A. borkumensis* ABS183 contains genes responsible for the reduction of

323   nitrogen oxides (KEGG genes: K00370-K00374 and K00362-K00363; nitrate reductase I

324   genes and nitrite reductase genes). The reduction process was believed to generate

325   ammonia for the efficient synthesis of amino acids (Schneiker et al., 2006). Ammonia

326   might be generated through nitrate reduction as indicated by the presence of the related

327 genes encoding nitrate and nitrite reduction enzymes (Fig. 6). Ammonia might be
328 imported by transmembrane transporters and assimilated into glutamate. A high demand
329 for fatty acids was a characteristic of *A. borkumensis* to perform rapid energy and organic
330 carbon storage. *A. borkumensis* ABS183 was probably able to synthesize long fatty acids
331 because the *fas* and *fabBFGIKZ* genes responsible for the elongation of fatty acids were
332 all present in its draft genome. In contrast, the essential *fas* gene (K11533) and other
333 relevant genes were not found in the control metagenome. Crude oil generally contains
334 aromatic compounds, and the current sediment at the sampling site also contained oil
335 (Wang et al., 2011). As expected, the two metagenomes possessed a complete set of
336 genes responsible for the degradation of aromatic compounds. Based on the homology of
337 the genes, the *Ochrobactrum* and *Alkanindiges* species probably played a role in this
338 degradation.

339

340 **3.4 Detection of bacteria in anhydrite crystals by DAPI and FISH**
341 To determine whether complete microbial cells could be maintained in the anhydrite
342 crystals, DAPI and FISH assays were conducted to visualize the microbes. The DAPI
343 results revealed the presence of complete cells that were released or embedded in the
344 crystals (Fig. 7A, D, and H). However, the FISH assay, which was used to detect *A.*
345 *borkumensis* ABS183 with two probes specific to the 16S rRNA gene, showed some
346 fluorescence-labeled microbes (Fig. 7B, E and I). These microbes could also be
347 envisioned with the FISH assay using the *alkB* gene probe (Fig. 7F and 7J). The *alkB* is
348 one of the functional genes that participate in alkane degradation (Schneiker et al., 2006).
349 The rod shape of the fluorescent microbes is consistent with the microscopic features
350 reported previously (Sabirova et al., 2011). These results indicated that some microbes in
351 the microscopic fields were *A. borkumensis* ABS183, as revealed in the anhydrite
352 metagenome.

353

354 **4 Discussion**
355 In the present study, we detected complete microbial cells and analyzed their
356 metagenome in the anhydrite crystals from a deep-sea anoxic basin. The dominant
357 bacterial species was *A. borkumensis* ABS183, an aerobic bacterium that is capable of

358   degrading alkanes in crude oil. *Alcanivorax* is one of the bacterial indicators for the
359   spilling of oil in waters and surface sediment (Yakimov et al., 2007). However, the
360   Atlantis II brine pool is anaerobic and increasingly hydrothermal (Bougouffa et al.,
361   2013b). The brine sediment in the basin was also found to be anoxic. Thus, *A.*
362   *borkumensis* ABS183 could not be current inhabitants of the hydrothermal anoxic basin.
363   This difference did not explain the stratification of microbial communities in the different
364   sediment layers of the brine-filled basin. A recent study showed that *Alcanivorax* was not
365   present in all sediment layers of a sediment core from the Atlantis II basin (Wang et al.,
366   2015). A reasonable explanation for this finding is that the anhydrite layer at 177-198 cm
367   in the sediment core was formed at a previous benthic site when hydrothermal solution
368   was injected into the seafloor. The organisms living in the benthic water and subsurface
369   sediment were subsequently sealed and protected in the anhydrite crystals. Because the
370   metabolism of *A. borkumensis* bacteria was specifically used for the degradation of
371   alkanes and other hydrocarbons in crude oil (Yakimov et al., 2007), the benthic site in
372   which the anhydrite layer formed was probably an oil-spilling or oil-forming environment
373   in the Atlantis II basin. The current hot sediments in the basin are biogenic and abiogenic
374   sources of crude oil (Simoneit, 1988). Seeping of the oil has resulted in proliferation of *A.*
375   *borkumensis* bacteria in the bottom water. Similarly, oil-utilizing bacteria were nourished
376   after the oil-spilling disaster in the Gulf of Mexico (Gutierrez et al., 2013). The *A.*
377   *borkumensis* bacteria were important producers of organic carbons as they could convert
378   alkanes and nitrate into organic matter. Fatty acids and lipopolysaccharides that were
379   yielded by *A. borkumensis* bacteria were nutrients for the whole ecosystem.

380

381   Based on the results in the present study, we propose that mild eruptions of hydrothermal
382   solutions injected calcium-rich solutions into the seafloor and produced anhydrite veins
383   by mixing with sulfate in the bottom water of the Atlantis II rift basin. The anhydrite
384   layer was then covered by sulfide minerals and biological debris such as the planktonic
385   foraminifera *G. sacculifer*. In this study, we narrowed the age of the thick anhydrite layer
386   to 750-770 years using ^{14}C isotope of the *G. sacculifer* specimens. This result also
387   indicates a relatively young sediment age and a high accumulation rate of precipitated
388   metals in the Atlantis II basin. Because the upward movement of hydrothermal solutions

389   might transfer some foraminifera specimens from lower layers to the anhydrite layer, we

390   did not use the foraminifera between anhydrite crystals. In our previous study, we have

391   shown evidence of oil formation in the Atlantis II brine pool (Wang et al., 2011). The

392   organic carbon content can be converted to aromatic compounds under the hydrothermal

393   conditions in the pool based on chemical and metagenomic evidence (Wang et al., 2011).

394   However, the bottom of the anoxic brine pool was not a habitat of *Alcanivorax* species

395   (Bougouffa et al., 2013a;Blanc and Anschutz, 1995), suggesting that *Alcanivorax*

396   flourished in the basin before the formation of brine water layers over the sediment

397   (Blanc and Anschutz, 1995).

398

399   Although there were differences in microbial communities between the anhydrite crystals

400   and the control sediment, *Ochrobactrum* sp. was one of the common inhabitants.

401   Previous studies have shown that *Ochrobactrum* species could metabolize aromatic

402   compounds aerobically and anaerobically (Zu et al., 2014;Mahmood et al., 2009), which

403   explains their presence in both metagenomes assessed in the current study. Moreover, we

404   determined the concentrations of nitrogen oxides in the different sulfide layers, although

405   only low concentrations were detected. *Ochrobactrum* species were potentially able to

406   anaerobically degrade polycyclic aromatic compounds using nitrate as an oxygen donor

407   (Mahmood et al., 2009;Wu et al., 2009). Such a chemolithoheterotrophic lifestyle is in

408   accordance with the current *in situ* environment of the sediment in the Atlantis II.

409   Regardless of the environmental changes indicated by the findings in the present study,

410   the spreading of *Ochrobactrum* sp. was seemingly not affected. Although the

411   metagenomes in the present study contained an abundant essential genes for degrading a

412   variety of aromatic compounds, the microbial degradation of these compounds might

413   have been attenuated by a lack of oxygen and a high level of salinity (Klinkhammer and

414   Lambert, 1989). Anaerobic degradation of compounds is more difficult than aerobic

415   degradation, often requiring oxygen donors such as nitrate and sulfate (Mahmood et al.,

416   2009;Wu et al., 2009). Based on its ability to survive under anoxic conditions,

417   *Ochrobactrum* sp. is probably able to maintain a higher level of fitness in the control

418   sediment compared with *Alcanivorax*. In the present study, the *Alkanindiges* identified in

419   both metagenomes was also a well-known alkane degrader (Klein et al., 2007;Bogan et

420   al., 2003). Because of its presence in both anhydrites and the adjacent sulfide layer, we

421   assumed that the *Alkanindiges* bacterium was also capable of surviving aerobically and

422   anaerobically in the oil-producing sediment. Hence, the change from an oxic to an anoxic

423   benthic environment caused a dramatic shift in the microbial communities, resulting in

424   the extinction of the obligate aerobic alkane-utilizer *Alcanivorax* and continuous

425   residency of anaerobic oil-degraders. The availability of nitrogen oxides and the

426   dissolution of sulfate from anhydrite crystals were possibly critical to the metabolic

427   activities of the anaerobes. In addition, the *Bacillus* and fungi present in the control

428   sediment were probably present in the form of dormant spores. In a recent report,

429   *Ochrobactrum* and *Bacillus* were confirmed to be dominant species in some upper sulfide

430   layers in the Atlantis II (Wang et al., 2015). Altogether, in the present study, the current

431   microbial inhabitants in the sulfide layers were largely different from those in the

432   anhydrite crystals.

433

434   The geochemical data collected herein suggested that the sub-superficial anhydrite layer

435   could release organic carbon contents into the sediment, as reported previously [12,13]. Our

436   measurement of DOC at 80.9 mg L^{-1} in the anhydrite layer was higher than the generally

437   accepted maximum value of 50 mg L^{-1} for marine sediments (Cameron et al., 2006). The

438   abnormally high DOC was considered a notable alteration of the local environments,

439   probably resulted from the breakdown of anhydrite crystals. Anhydrites in the Atlantis II

440   brine sediment were likely maintained by the high salinity and temperature, and then

441   slowly dissolved. This phenomenon may be explained by the slight undersatuation of the

442   anhydrite in the Atlantis II sediment (Anschutz et al., 2000). Such anhydrite layers are

443   widely distributed in Middle Eastern sediments (Alsharhan and Nairn, 1997). Hence, our

444   findings shed light on the formation of micro-environments by anhydrite evaporites in the

445   deep sediments. In this study, there was an inconsistency between the cell density and the

446   DOC at the 12-cm depth layer, in which the DOC could not support a 10-fold higher

447   biomass. This phenomenon probably resulted from the formation of petroleum

448   compounds under the hydrothermal effects (Wang et al., 2011). In the petroleum,

449   hydrophobic organic compounds (HOCs) consisting of polycyclic aromatic hydrocarbons

450   (PAHs) could not be counted in our DOC measurements (personal communication with J.

451 Pearsons). The nutrient supply is critical for microbes to survive in deep-sea sediment.
452 Apart from the chemolithoautotrophic microbes, numerous other inhabitants take
453 advantage of the buried organic matter. Importantly, the trapped organic matter serves as
454 a nutrient supply following the dissolution of organic-rich anhydrite crystals. Therefore,
455 our findings highlighted the importance of the nutrients released from the anhydrite facies
456 for microbes in deep-sea subsuperficial sediment.
457

458 *Author contributions.* Y. Wang, T.G. Li, and P. Y. Qian were responsible for the study
459 design. Data analysis was performed by Y. Wang, T.G. Li, J. T. Li, Q. L. Lai, and Z. M.
460 Gao. M.Y. Wang conducted FISH assay. The manuscript was prepared by Y. Wang with
461 contributions from all co-authors.

462 *Acknowledgments.* This study was supported by the National Science Foundation of
463 China No. 41476104 and No. 31460001 to Y. Wang, and the King Abdullah University
464 of Science and Technology (SA-C0040/UK-C0016) to P.Y. Qian. This work was also
465 supported by Hainan international collaborative grant No. KJHZ2015-22.

466

References

468 Albertsen, M., Hugenholtz, P., Skarshewski, A., Nielsen, K. L., Tyson, G. W., and
469   Nielsen, P. H.: Genome sequences of rare, uncultured bacteria obtained by differential
470   coverage binning of multiple metagenomes, Nat Biotechnol, 31, 533-538, Doi
471   10.1038/Nbt.2579, 2013.
472 Alsharhan, A. S., and Nairn, A. E. M.: Sedimentary basins and petroleum geology of the
473   Middle East, Elsevier Science B.V., Amsterdam, 1997.
474 Anschutz, P., and Blanc, G.: Heat and salt fluxes in the Atlantis II Deep (Red Sea), Earth
475   Planet Sci Lett, 142, 147-159, 1996.
476 Anschutz, P., Blanc, G., Monnin, C., and Boulègue, J.: Geochemical dynamics of the
477   Atlantis II Deep (Red Sea): II. Composition of metalliferous sediment pore waters,
478   Geochim Cosm Acta, 64, 3995-4006, 2000.
479 Auch, A. F., Klenk, H. P., and Goker, M.: Standard operating procedure for calculating
480   genome-to-genome distances based on high-scoring segment pairs, Stand Genomic Sci,
481   2, 142-148, 10.4056/sigs.541628, 2010a.
482 Auch, A. F., von Jan, M., Klenk, H. P., and Goker, M.: Digital DNA-DNA hybridization
483   for microbial species delineation by means of genome-to-genome sequence comparison,
484   Stand Genomic Sci, 2, 117-134, 10.4056/sigs.531120, 2010b.
485 Babel, M.: Models for evaporite, selenite and gypsum microbialite deposition in ancient
486   saline basins, Acta Geologica Polonica, 54, 219-249, 2004.
487 Bard, E.: Correction of accelerator mass spectrometry 14C ages measured in planktonic
488   foraminifera: Paleoceanographic implications., Paleoceanography, 3, 635-645, 1988.
489 Barret, M., Gagnon, N., Morissette, B., Topp, E., Kalmokoff, M., Brooks, S. P. J., Matias,
490   F., Massé, D. I., Masse, L., and Talbot, G.: Methanoculleus spp. as a biomarker of
491   methanogenic activity in swine manure storage tanks, FEMS Microbiol Eco, 80,
492   427-440, 10.1111/j.1574-6941.2012.01308.x, 2012.
493 Benison, K. C., Jagniecki, E. A., Edwards, T. B., Mormile, M. R., and Storrie-Lombardi,
494   M. C.: "Hairy blobs:" microbial suspects preserved in modern and ancient extremely
495   acid lake evaporites, Astrobiology, 8, 807-821, 10.1089/ast.2006.0034, 2008.
496 Blanc, G., and Anschutz, P.: New stratification in the hydrothermal brine system of the
497   Atlantis II Deep, Red Sea, Geology, 23, 543-546, 1995.
498 Bogan, B. W., Sullivan, W. R., Kayser, K. J., Derr, K. D., Aldrich, H. C., and Paterek, J.
499   R.: Alkanindiges illinoisensis gen. nov., sp. nov., an obligately hydrocarbonoclastic,
500   aerobic squalane-degrading bacterium isolated from oilfield soils, Int J Syst Evol
501   Microbiol, 53, 1389-1395, 10.1099/ijs.0.02568-0, 2003.
502 Bougouffa, S., Yang, J. K., Lee, O. O., Wang, Y., Batang, Z., Al-Suwailem, A., and Qian,
503   P. Y.: Distinctive microbial community structure in highly stratified deep-sea brine
504   water columns, Appl Environ Microbiol, 79, 3425-3437, 10.1128/aem.00254-13, 2013a.
505 Bougouffa, S., Yang, J. K., Lee, O. O., Wang, Y., Batang, Z., Al-Suwailem, A., and
506   Qiana, P. Y.: Distinctive microbial community structure in highly stratified deep-sea
507   brine water columns, Appl Environ Microb, 79, 3425-3437, Doi
508   10.1128/Aem.00254-13, 2013b.
509 Bower, A. S.: R/V Oceanus Voyage 449-6 Red Sea Atlantis II Deep Complex Area 19
510   October-1 November 2008, Woods Hole Oceanographic Institution, 2009.

511 Brocks, J. J., Love, G. D., Summons, R. E., Knoll, A. H., Logan, G. A., and Bowden, S.
512   A.: Biomarker evidence for green and purple sulphur bacteria in a stratified
513   Palaeoproterozoic sea, Nature, 437, 866-870, 2005.
514 Cameron, D., Willett, M., and Hammer, L.: Distribution of organic carbon in the
515   Berkeley Pit lake, Butte, Montana, Mine Water Environ, 25, 93-99,
516   10.1007/s10230-006-0116-4, 2006.
517 Dupraz, C., Reid, R. P., and Visscher, P. T.: Microbialites, modern, in: Encyclopaedia of
518   Geobiology, edited by: Reitner, V., and Thiel, J., Springer, Heidelberg, 617-635, 2011.
519 Girdler, R. W.: A review of Red Sea heat flow, Phil Trans Roy Soc Lon A, 267, 191-203,
520   1970.
521 Goris, J., Konstantinidis, K. T., Klappenbach, J. A., Coenye, T., Vandamme, P., and
522   Tiedje, J. M.: DNA–DNA hybridization values and their relationship to whole-genome
523   sequence similarities, Int J Syst Evol Microbiol, 57, 81-91, 2007.
524 Gough, H. L., and Stahl, D. A.: Optimization of direct cell counting in sediment. , J
525   Microbiol Methods, 52, 39-46, 2003.
526 Gutierrez, T., Singleton, D. R., Berry, D., Yang, T., Aitken, M. D., and Teske, A.:
527   Hydrocarbon-degrading bacteria enriched by the Deepwater Horizon oil spill identified
528   by cultivation and DNA-SIP, ISME J, 7, 2091-2104, 10.1038/ismej.2013.98, 2013.
529 Hill, A. E.: The transition temperature of gypsum to anhydrite, J Am Chem Soc, 59,
530   2242-2244, 10.1021/ja01290a039, 1937.
531 Huang, Y., Gilna, P., and Li, W.: Identification of ribosomal RNA genes in metagenomic
532   fragments, Bioinformatics, 25, 1338-1340, 2009.
533 Hyatt, D., Chen, G. L., LoCascio, P. F., Land, M. L., Larimer, F. W., and Hauser, L. J.:
534   Prodigal: prokaryotic gene recognition and translation initiation site identification,
535   BMC Bioinformatics, 11, Artn 119 Doi 10.1186/1471-2105-11-119, 2010.
536 Jannasch, H. W., and Mottl, M. J.: Geomicrobiology of deep-sea hydrothermal vents,
537   Science, 229, 717-725, 10.1126/science.229.4715.717, 1985.
538 Kanehisa, M., Goto, S., Sato, Y., Furumichi, M., and Tanabe, M.: KEGG for integration
539   and interpretation of large-scale molecular data sets, Nucleic Acids Res, 40, D109-114,
540   10.1093/nar/gkr988, 2012.
541 Kim, O. S., Cho, Y. J., Lee, K., Yoon, S. H., Kim, M., Na, H., Park, S. C., Jeon, Y. S.,
542   Lee, J. H., Yi, H., Won, S., and Chun, J.: Introducing EzTaxon-e: a prokaryotic 16S
543   rRNA gene sequence database with phylotypes that represent uncultured species, Int J
544   Syst Evol Microbiol, 62, 716-721, 10.1099/ijs.0.038075-0, 2012.
545 Klein, A. N., Frigon, D., and Raskin, L.: Populations related to Alkanindiges, a novel
546   genus containing obligate alkane degraders, are implicated in biological foaming in
547   activated sludge systems, Environ Microbiol, 9, 1898-1912,
548   10.1111/j.1462-2920.2007.01307.x, 2007.
549 Klinkhammer, G. P., and Lambert, C. E.: Preservation of organic matter during salinity
550   excursions, Nature, 339, 271-274, 1989.
551 Kristall, B., Kelley, D. S., Hannington, M. D., and Delaney, J. R.: Growth history of a
552   diffusely venting sulfide structure from the Juan de Fuca Ridge: A petrological and
553   geochemical study, Geochem. Geophys. Geosyst., 7, Q07001, 10.1029/2005gc001166,
554   2006.

555 Li, H., Handsaker, B., Wysoker, A., Fennell, T., Ruan, J., Homer, N., Marth, G., Abecasis,
556   G., and Durbin, R.: The sequence alignment/map format and SAMtools, Bioinformatics,
557   25, 2078-2079, DOI 10.1093/bioinformatics/btp352, 2009.
558 Ludwig, W., Strunk, O., Westram, R., Richter, L., Meier, H., Yadhukumar, Buchner, A.,
559   Lai, T., Steppi, S., Jobb, G., Forster, W., Brettske, I., Gerber, S., Ginhart, A. W., Gross,
560   O., Grumann, S., Hermann, S., Jost, R., Konig, A., Liss, T., Lussmann, R., May, M.,
561   Nonhoff, B., Reichel, B., Strehlow, R., Stamatakis, A., Stuckmann, N., Vilbig, A.,
562   Lenke, M., Ludwig, T., Bode, A., and Schleifer, K.-H.: ARB: a software environment
563   for sequence data, Nucleic Acids Res., 32, 1363-1371, 10.1093/nar/gkh293, 2004.
564 Mahmood, Q., Hu, B., Cai, J., Zheng, P., Azim, M. R., Jilani, G., and Islam, E.: Isolation
565   of Ochrobactrum sp.QZ2 from sulfide and nitrite treatment system, J Hazardous
566   Materials, 165, 558-565, 2009.
567 Meier-Kolthoff, J. P., Auch, A. F., Klenk, H. P., and Goker, M.: Genome sequence-based
568   species delimitation with confidence intervals and improved distance functions, BMC
569   bioinformatics, 14, 60, 10.1186/1471-2105-14-60, 2013.
570 Missack, E., Stoffers, P., and El Goresy, A.: Mineralogy, paragenesis, and phases
571   relations of copper iron sulfides in the Atlantis II Deep, Red Sea, Min. Deposita, 24,
572   82-91, 1989.
573 Nurk, S., Bankevich, A., Antipov, D., Gurevich, A. A., Korobeynikov, A., Lapidus, A.,
574   Prjibelski, A. D., Pyshkin, A., Sirotkin, A., Sirotkin, Y., Stepanauskas, R., Clingenpeel,
575   S. R., Woyke, T., McLean, J. S., Lasken, R., Tesler, G., Alekseyev, M. A., and Pevzner,
576   P. A.: Assembling single-cell genomes and mini-metagenomes from chimeric MDA
577   products, J Comput Biol, 20, 714-737, 10.1089/cmb.2013.0084, 2013.
578 Orcutt, B. N., Sylvan, J. B., Knab, N. J., and Edwards, K. J.: Microbial ecology of the
579   dark ocean above, at, and below the seafloor, Microbiol Mol Biol Rev, 75, 361-422, Doi
580   10.1128/Mmbr.00039-10, 2011.
581 Oudin, E., Thisse, Y., and Ramboz, C.: Fluid inclusion and mineralogical evidence for
582   high temperature saline hydrothermal circulation in the Red Sea metalliferous sediments:
583   preliminary results, Mar. Mining, 5, 3-31, 1984.
584 Overbeek, R., Begley, T., Butler, R. M., Choudhuri, J. V., Chuang, H. Y., Cohoon, M., de
585   Crecy-Lagard, V., Diaz, N., Disz, T., Edwards, R., Fonstein, M., Frank, E. D., Gerdes,
586   S., Glass, E. M., Goesmann, A., Hanson, A., Iwata-Reuyl, D., Jensen, R., Jamshidi, N.,
587   Krause, L., Kubal, M., Larsen, N., Linke, B., McHardy, A. C., Meyer, F., Neuweger, H.,
588   Olsen, G., Olson, R., Osterman, A., Portnoy, V., Pusch, G. D., Rodionov, D. A.,
589   Ruckert, C., Steiner, J., Stevens, R., Thiele, I., Vassieva, O., Ye, Y., Zagnitko, O., and
590   Vonstein, V.: The subsystems approach to genome annotation and its use in the project
591   to annotate 1000 genomes, Nucleic Acids Res, 33, 5691-5702, 33/17/5691 [pii]
592   10.1093/nar/gki866, 2005.
593 Parkes, R. J., Cragg, B. A., and Wellsbury, P.: Recent studies on bacterial populations
594   and processes in subseafloor sediments: A review, Hydrogeol J, 8, 11-28,
595   10.1007/pl00010971, 2000.
596 Party, T. S. S.: Red Sea: Site 226, in: Deep Sea Drilling Project, 595-600, 1974.
597 Pernthaler, A., Pernthaler, J., and Amann, R.: Fluorescence in situ hybridization and
598   catalyzed reporter deposition for the identification of marine bacteria, Appl Environ
599   Microb, 68, 3094-3101, 2002.

Petrash, D. A., Gingras, M. K., Lalonde, S. V., Orange, F., Pecoits, E., and Konhauser, K. O.: Dynamic controls on accretion and lithification of modern gypsum-dominated thrombolites, Los Roques, Venezuela, Sedi Geol, 245-246, 29-47, 2012.

Quast, C., Pruesse, E., Yilmaz, P., Gerken, J., Schweer, T., Yarza, P., Peplies, J., and Glöckner, F. O.: The SILVA ribosomal RNA gene database project: improved data processing and web-based tools, Nucleic Acids Res, 41, D590-D596, 10.1093/nar/gks1219, 2013.

Ramboz, C., Oudin, E., and Thisse, Y.: Geyser-type discharge in Atlantis II Deep, Red Sea: evidence of boiling from fluid inclusions in epigenetic anhydrite, Can Mineral, 26, 765-786, 1988.

Reimer, P. J., Baillie, M. G. L., Bard, E., Bayliss, A., Beck, J. W., Blackwell, P. G., Ramsey, C. B., Buck, C. E., Burr, G. S., Edwards, R. L., Friedrich, M., Grootes, P. M., Guilderson, T. P., Hajdas, I., Heaton, T. J., Hogg, A. G., Hughen, K. A., Kaiser, K. F., Kromer, B., McCormac, F. G., Manning, S. W., Reimer, R. W., Richards, D. A., Southon, J. R., Talamo, S., Turney, C. S. M., van der Plicht, J., and Weyhenmeyer, C. E.: IntCal09 and Marine09 radiocarbon age calibration curves, 0-50,000yeats cal BP, Radiocarbon, 51, 1111-1150, 2009.

Richter, M., and Rosselló-Mora, R.: Shifting the genomic gold standard for the prokaryotic species definition, Proc Natl Acad Sci U S A, 106, 19126-19131, 10.1073/pnas.0906412106, 2009.

Sabirova, J. S., Becker, A., Lunsdorf, H., Nicaud, J. M., Timmis, K. N., and Golyshin, P. N.: Transcriptional profiling of the marine oil-degrading bacterium Alcanivorax borkumensis during growth on n-alkanes, FEMS Microbiol Lett, 319, 160-168, 10.1111/j.1574-6968.2011.02279.x, 2011.

Schardt, C.: Hydrothermal fluid migration and brine pool formation in the Red Sea: the Atlantis II Deep, Mineralium Deposita, 51, 89-111, 10.1007/s00126-015-0583-2, 2016.

Schloss, P. D., Westcott, S. L., Ryabin, T., Hall, J. R., Hartmann, M., Hollister, E. B., Lesniewski, R. A., Oakley, B. B., Parks, D. H., Robinson, C. J., Sahl, J. W., Stres, B., Thallinger, G. G., Van Horn, D. J., and Weber, C. F.: Introducing mothur: Open-source, platform-independent, community-supported software for describing and comparing microbial communities, Appl Env Microbiol, 75, 7537-7541, 10.1128/aem.01541-09, 2009.

Schneiker, S., Martins dos Santos, V. A., Bartels, D., Bekel, T., Brecht, M., Buhrmester, J., Chernikova, T. N., Denaro, R., Ferrer, M., Gertler, C., Goesmann, A., Golyshina, O. V., Kaminski, F., Khachane, A. N., Lang, S., Linke, B., McHardy, A. C., Meyer, F., Nechitaylo, T., Puhler, A., Regenhardt, D., Rupp, O., Sabirova, J. S., Selbitschka, W., Yakimov, M. M., Timmis, K. N., Vorholter, F. J., Weidner, S., Kaiser, O., and Golyshin, P. N.: Genome sequence of the ubiquitous hydrocarbon-degrading marine bacterium Alcanivorax borkumensis, Nature Biotech, 24, 997-1004, 10.1038/nbt1232, 2006.

Simoneit, B. R. T.: Petroleum generation submarine hydrothermal systems: An update, Can Mineral, 26, 827-840, 1988.

Swallow, J. C., and Crease, J.: Hot salty water at the bottom of the Red Sea, Nature, 205, 165-166, 1965.

Taher, A. G.: Microbially induced sedimentary structures in evaporite–siliciclastic sediments of Ras Gemsa sabkha, Red Sea Coast, Egypt, J Adv Res, 5, 577-586, 2014.

645   Tamura, K., Peterson, D., Peterson, N., Stecher, G., Nei, M., and Kumar, S.: MEGA5:
646   molecular evolutionary genetics analysis using maximum likelihood, evolutionary
647   distance, and maximum parsimony methods, Mol Biol Evol, 28, 2731-2739, 2011.
648   Teske, A., and Sorensen, K. B.: Uncultured archaea in deep marine subsurface sediments:
649   have we caught them all?, ISME J, 2, 3-18, 2007.
650   Trichet, J., Défarge, C., Tribble, J., Tribble, G. W., and Sansone, F. J.: Christmas Island
651   lagoonal lakes, models for the deposition of carbonate-evaporite-organic laminated
652   sediments, Sedimentary Geol, 140, 177-189, 2001.
653   Wang, W., Wang, L., and Shao, Z.: Diversity and abundance of oil-degrading bacteria
654   and alkane hydroxylase (alkB) genes in the subtropical seawater of Xiamen Island,
655   Microb Ecol, 60, 429-439, 10.1007/s00248-010-9724-4, 2010.
656   Wang, Y., Yang, J., Lee, O. O., Dash, S., Lau, S. C. K., Al-Suwailem, A., Wong, T. Y. H.,
657   Danchin, A., and Qian, P.-Y.: Hydrothermally generated aromatic compounds are
658   consumed by bacteria colonizing in Atlantis II Deep of the Red Sea, ISME J, 5, 1652–
659   1659, 2011.
660   Wang, Y., Li, J. T., He, L. S., Yang, B., Gao, Z. M., Cao, H. L., Batang, Z., Al-Suwailem,
661   A., and Qian, P. Y.: Zonation of microbial communities by a hydrothermal mound in
662   the Atlantis II Deep (the Red Sea), PLoS ONE, 10, e0140766,
663   10.1371/journal.pone.0140766, 2015.
664   Wang, Y., Gao, Z. M., Xu, Y., Li, G. Y., He, L. S., and Qian, P. Y.: An evaluation of
665   multiple annealing and looping based genome amplification using a synthetic bacterial
666   community, ACTA Oceanol Sin, 35, 131-136, 2016.
667   Wayne, L. G., Brenner, D. J., Colwell, R. R., Grimont, P. A. D., Kandler, O., Krichevsky,
668   M. I., Moore, L. H., Moore, W. E. C., Murray, R. G. E., Stackebrandt, E., Starr, M. P.,
669   and Trüper, H. G.: Report of the ad hoc committee on reconciliation of approaches to
670   bacterial systematics, Int J Syst Evol Microbiol,, 37, 463-464, 1987.
671   Webster, G., John Parkes, R., Cragg, B. A., Newberry, C. J., Weightman, A. J., and Fry, J.
672   C.: Prokaryotic community composition and biogeochemical processes in deep
673   subseafloor sediments from the Peru Margin, FEMS Microbiol Ecol, 58, 65-85,
674   10.1111/j.1574-6941.2006.00147.x, 2006.
675   Wu, Y., He, T., Zhong, M., Zhang, Y., Li, E., Huang, T., and Hu, Z.: Isolation of marine
676   benzo[a]pyrene-degrading Ochrobactrum sp. BAP5 and proteins characterization, J
677   Environ Sci, 21, 1446-1451, 2009.
678   Yakimov, M. M., Timmis, K. N., and Golyshin, P. N.: Obligate oil-degrading marine
679   bacteria, Curr Opin Biotech, 18, 257-266, 2007.
680   Zierenberg, R. A., and Shanks, W. C.: Mineralogy and geochemistry of epigenetic
681   features in metalliferous sediment, Atlantis II Deep, Red Sea, Econ Geol, 78, 57-72,
682   10.2113/gsecongeo.78.1.57, 1983.
683   Zong, C., Lu, S., Chapman, A. R., and Xie, X. S.: Genome-wide detection of
684   single-nucleotide and copy-number variations of a single human cell, Science, 338,
685   1622-1626, 10.1126/science.1229164, 2012.
686   Zu, L., Xiong, J., Li, G., Fang, Y., and An, T.: Concurrent degradation of
687   tetrabromobisphenol A by Ochrobactrum sp. T under aerobic condition and estrogenic
688   transition during these processes, Ecotoxicol Environ Safety, 104, 220-225,
689   10.1016/j.ecoenv.2014.03.015, 2014.
690

691 **Data Accessibility**

692 Illumina raw data will be accessible under SRA356974 in the NCBI SRA database. *A.*

693 *borkumensis* ABS183 genome was deposited at the NCBI database: BioProject

694 LKAP00000000.

695

696

697 **Table 1.** Age estimates of the sediment layers

Layer (cm)	Age (year)	Age error (year)
3-6	320	25
21-24	475	35
45-48	490	30
90-93	500	25
129-132	560	35
153-156	750	30
198-201	770	30
222-225	880	30

698

699 Eight sediment layers were selected for the age estimates using radioisotope ^{14}C of *G.*

700 *sacculifer* collected from the respective layers. The age was corrected by the 400-year

701 reservoir age with an error range.

702

703

704   **Figures**

705   **Figure 1. Anhydrite crystals and genome binning.**

706   Anhydrite crystals in a Petri dish (90 mm in diameter) (A) were used for DNA extraction.

707   The amplified genomic DNA was sequenced and then reassembled. Based on the G+C

708   content and read coverage, the binned contigs with high coverage levels (B) were

709   selected for examination of the tetranucleotide frequency consistency in the PCA analysis

710   (C).

711

712
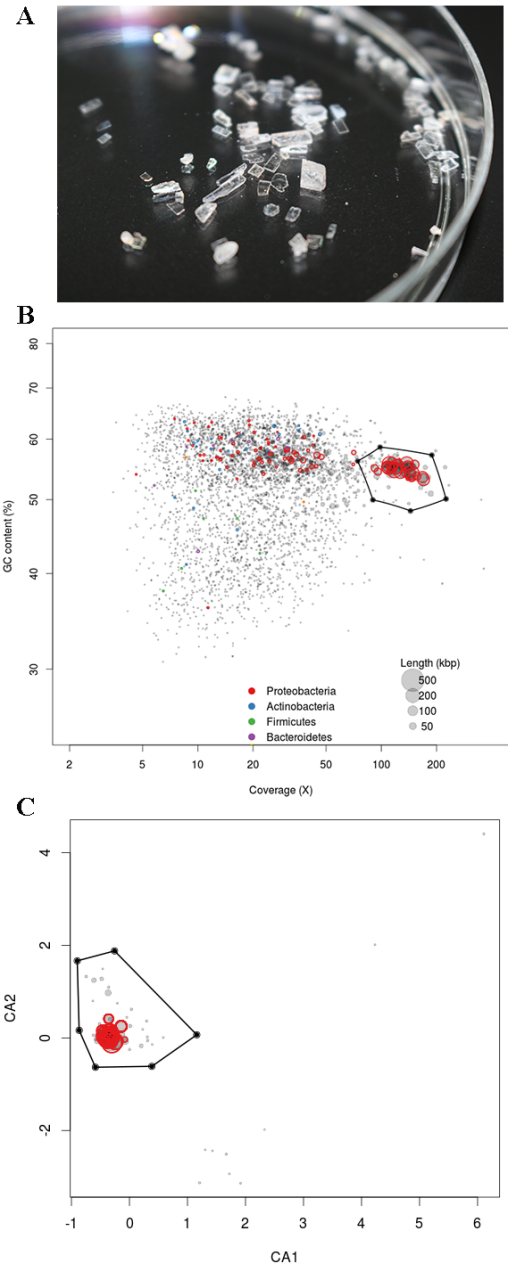
Figure 2. Grain size and age of selected layers

The percentages of the small particles (<63μm) in dry weight are shown for 75 slices of the sediment core (small squares on the line). The age estimates (black circles) of the selected layers were performed using radioisotope 14C of the monospecific *Globigerinoides sacculifer* specimens. Age errors ranged between 25 to 40 years. Anhydrite and control layers for metagenomic study were indicated by arrows.

719

720

721
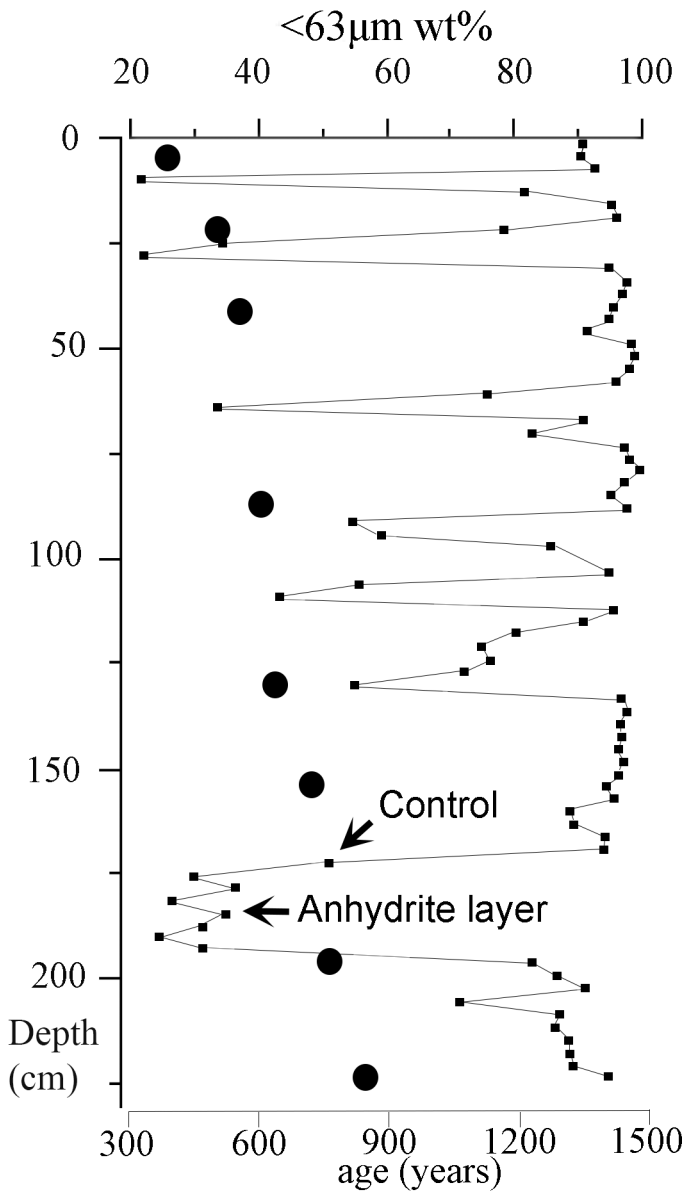
722 **Figure 3. Nutrient measurements and cell counts in the different sediment layers.**

723 The pore water samples were analyzed for five layers of a sediment core obtained from

724 the Atlantis II Deep (21°20.76' N, 38°04.68' E) in 2008. DOC: dissolved organic carbon.

725

726

727

728

729

730

731

732

733

734

735

736

737

738

739

740

741

742
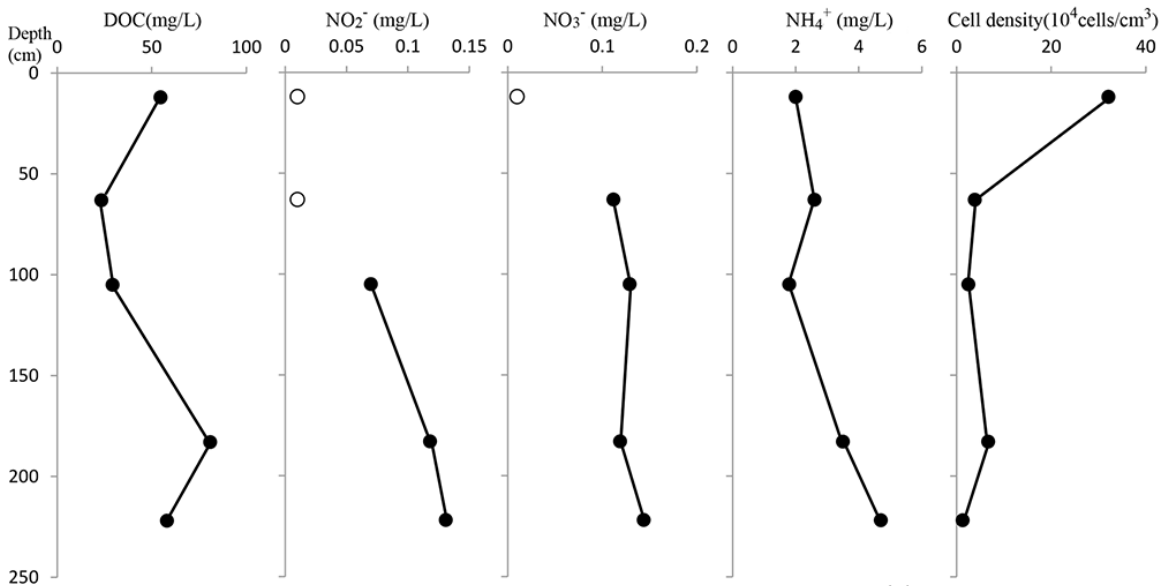
743 **Figure 4. Microbial communities in anhydrite crystals and neighboring control**

744 **sediment.**

745 Phyla and genera in the anhydrite crystals and control layer were predicted using 16S/18S

746 rRNA gene fragments extracted from the corresponding metagenomes (D-T:

747 Deinococcus-Thermus). The relative abundance of the genera can be estimated by the

748 coverage level (>5) of the 16S/18S rRNA fragments by reads.

749

750

751

752

753

754

755

756

757
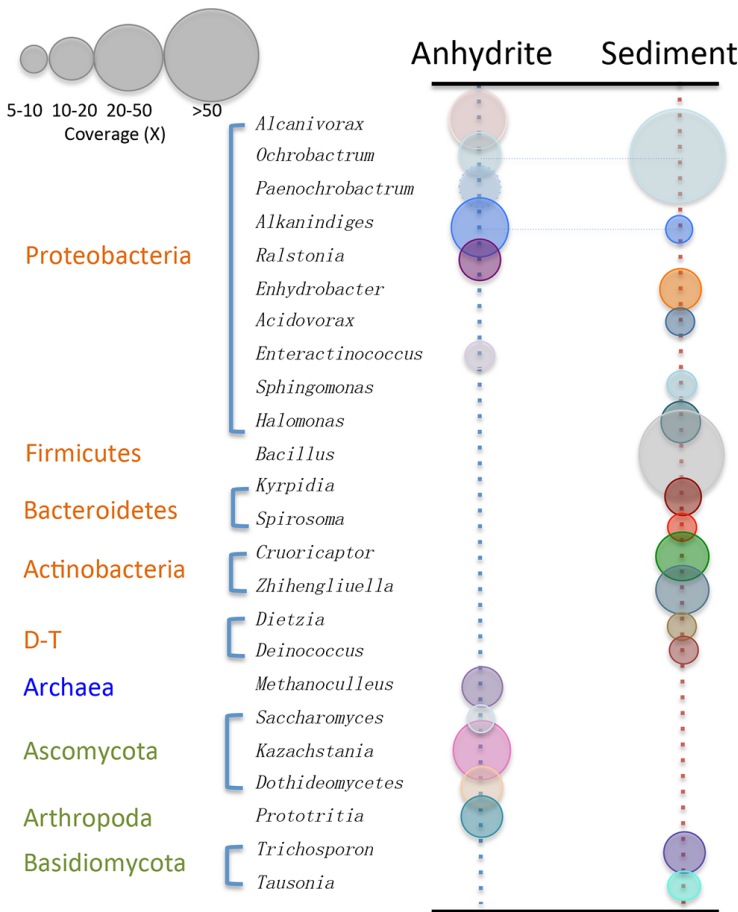
758 **Figure 5. Phylogenetic tree of 16S rRNA genes.**

759 Bootstrap values (expressed as percentages of 1000 replications) are shown at the

760 branches of the neighbor-joining tree.

761

762
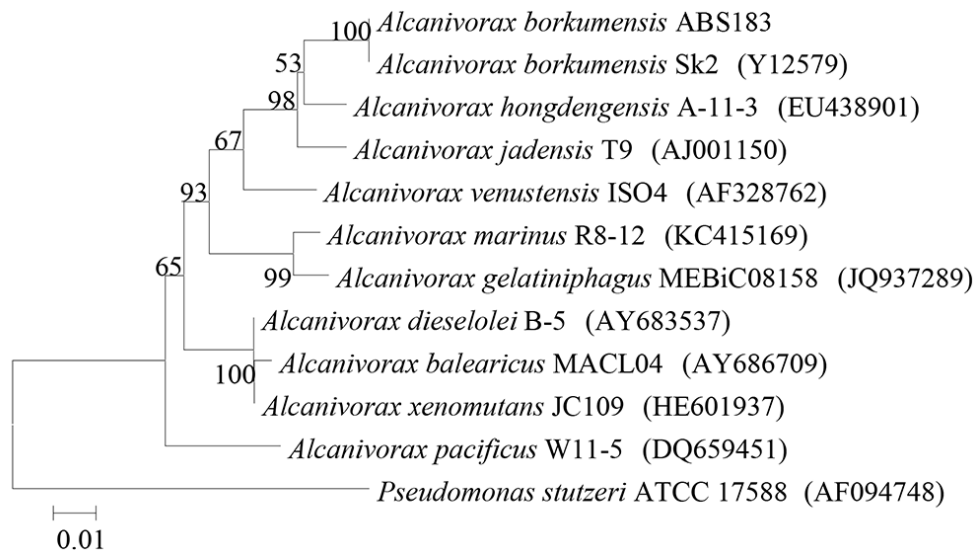
763 **Figure 6. Schematic model of metabolism and cross-membrane transporters**

764 The model was predicted based on the genes in the draft genome of *Alcanivorax*

765 *borkumensis* ABS183.

766

767

768

769
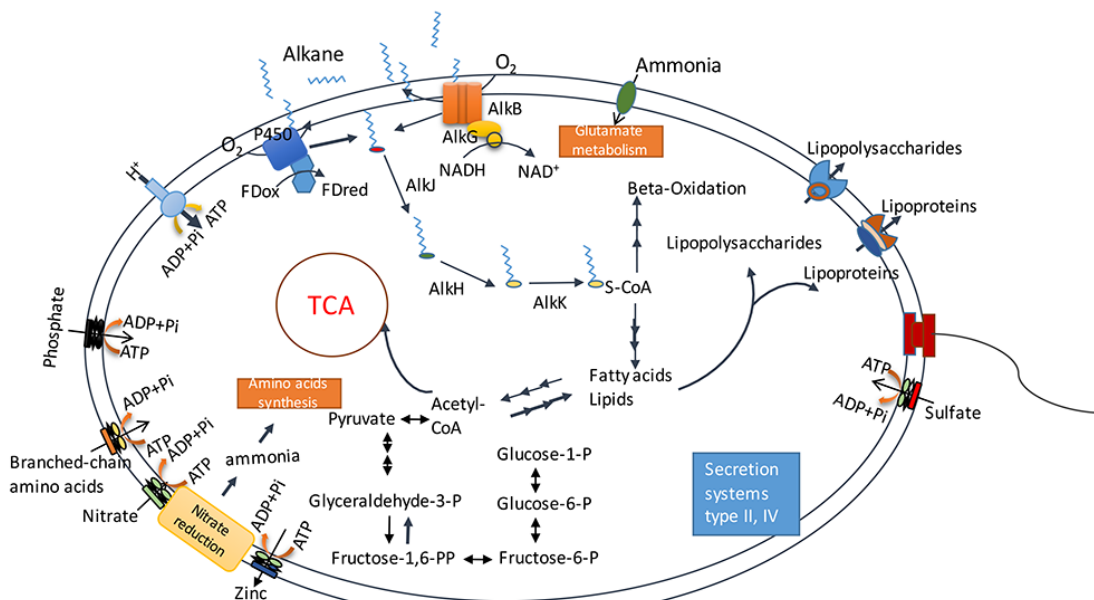
Figure 7. Fluorescence *in situ* hybridization (FISH) of *Alcanivorax* sp. ABS183 embedded in anhydrite crystals.

DAPI staining and FISH using 16S rRNA probes are shown in A and B. The merged image of A and B is shown in Fig. 7C. DAPI staining and FISH were also performed using two samples that were filtered with 3-μm (D-G) and 0.22-μm (H-K) membranes, respectively. *Alcanivorax* bacteria were released from the large crystals filtered through the 3-μm membranes (D-G). The bacteria were stained with DAPI (D), 16S rRNA probes (E) and the *alkB* probe (F), respectively, and overlaid (G). Using a sample filtered through a 0.22-μm membrane, a dividing *Alcanivorax* sp. ABS183 cell was labeled using the same method and probes (H-J). The microscopic fields shown in H-J are merged in Fig. 7K.

780

781

782